

## ENERGY SPECTRA OF IONS ACCELERATED IN IMPULSIVE AND GRADUAL SOLAR EVENTS

D. V. REAMES, L. M. BARBIER, AND T. T. VON ROSENVINGE  
NASA/Goddard Space Flight Center, Greenbelt, MD 20771

AND

G. M. MASON, J. E. MAZUR, AND J. R. DWYER  
University of Maryland, College Park, MD 20742

Received 1996 September 20; accepted 1997 January 16

### ABSTRACT

We report new high-sensitivity measurements of the energy spectra of ions from five impulsive solar flares and one gradual event observed during solar minimum by the Energetic Particles, Acceleration, Composition, and Transport (EPACT) experiment aboard the *WIND* spacecraft. All of the impulsive-flare events had intensities too low to be visible on previous spacecraft such as *ISEE 3*, which observed hundreds of impulsive-flare events. Often these events cluster in or behind a coronal mass ejection (CME) where magnetic field lines provide an excellent connection to a solar active region where flares are occurring. In most cases we can see velocity dispersion as the ions of 20 keV  $\text{amu}^{-1}$  to 10 MeV  $\text{amu}^{-1}$  streamed out from the impulsive flare at the Sun, arriving in inverse order of their velocity. Ions from a large, magnetically well-connected gradual event, associated with a CME-driven shock, also show velocity dispersion early in the event but show identical time profiles that last for several days late in the event. These time-invariant spectra of H,  $^4\text{He}$ , C, O, and Fe in this gradual event are well represented as power laws in energy from 20 keV  $\text{amu}^{-1}$  to  $\sim 100$  MeV  $\text{amu}^{-1}$ . In the impulsive-flare events, H,  $^3\text{He}$ ,  $^4\text{He}$ , C, O, and Fe have more rounded spectra that flatten somewhat at low energies; yet the intensities continue to increase down to 20 keV  $\text{amu}^{-1}$ . Most of the ion energy content appears to lie below 1 MeV in the impulsive events, where it would be invisible to  $\gamma$ -ray line observations.

*Subject headings:* Sun: flares — Sun: particle emission

### 1. INTRODUCTION

During the last decade we have discovered that ions accelerated in impulsive solar flares have characteristic abundance enhancements, e.g.,  $^3\text{He}/^4\text{He} \sim 1$  and  $\text{Fe}/\text{O} \sim 1$ , that unambiguously distinguish these particles from the normal coronal abundances found for ions accelerated by CME-driven shocks in large proton events (see reviews by Reames 1990; 1993, 1995a; Gosling 1993). The usual abundances are evidently produced when the ions resonantly absorb waves produced by beams of streaming electrons (Temerin & Roth 1993; Miller & Viñas 1993) or other waves (e.g., Zhang & Ohsawa 1995; Zhang 1995; Miller & Reames 1996) produced in the flare plasma. Element abundances have been measured in a large number of impulsive-flare events (Mason et al. 1986; Reames, Meyer, & von Rosenvinge 1994), and similar abundances have been deduced for the energetic ion beam that interacts to produce broad  $\gamma$ -ray lines in flare loops (Murphy et al. 1991). The association of the energetic ions with electrons and with radio, X-ray, and  $\text{H}\alpha$  emission in a large number of individual impulsive flares has been fully documented (Reames, von Rosenvinge, & Lin 1985; Reames & Stone 1986; Reames et al. 1988; Reames, Cane, & von Rosenvinge 1990), and the transport of the particles from the Sun has been studied (e.g., Mason et al. 1989).

Early measurements of spectra of  $^3\text{He}$ ,  $^4\text{He}$ , O, and Fe ions from 0.5 to  $\sim 10$  MeV  $\text{amu}^{-1}$  in impulsive-flare events were made by Möbius et al. (1982). These authors found the spectra to be consistent with a model of stochastic acceleration by wave turbulence. However, time periods of several days, often containing multiple flares, were summed to

produce these spectra. Van Hollebeke, McDonald, & Meyer (1990) measured spectra of elements up through Fe from  $\sim 1$  to  $\sim 100$  MeV  $\text{amu}^{-1}$  in two very large impulsive-flare events. In such large events, however, it is possible that shock acceleration contributes additional acceleration. Despite a lack of resolution of ion species below 0.5 MeV  $\text{amu}^{-1}$ , Reames, Richardson, & Wenzel (1992) attempted to extrapolate the observed abundances, using differences in the ion arrival times, to extend  $^4\text{He}$  and H spectra down to  $\sim 100$  keV  $\text{amu}^{-1}$ . They found interesting evidence for flattening in the  $^4\text{He}$  spectra at low energies in several events. More recently, Mazur, Mason, & Klecker (1995) resolved ion species from  $\sim 0.5$  to  $\sim 20$  MeV  $\text{amu}^{-1}$ . They reported that  $^3\text{He}$ ,  $^4\text{He}$ , and ions up through Fe all had similar power-law spectra. Unfortunately, these authors were also forced to integrate the spectra over several days containing several individual flares.

Meanwhile, the importance of obtaining good-quality ion spectra in impulsive flares has been highlighted by recent measurements of  $\gamma$ -ray lines (Share & Murphy 1995; Ramaty et al. 1995). The strong Ne line at 1.63 MeV and its variation from event to event can be best understood in terms of steep, but variable, ion spectra in these events. These steep spectra also suggest that ions, rather than electrons, can contain most of the energy in accelerated particles in some flares. While these  $\gamma$ -ray line measurements have provided important spectral information using line strengths at several discrete energies, such measurements cannot determine the complete spectrum of any particular ion species, the mix of energetic ions present, or any spectral differences between species. Furthermore,  $\gamma$ -ray line spec-

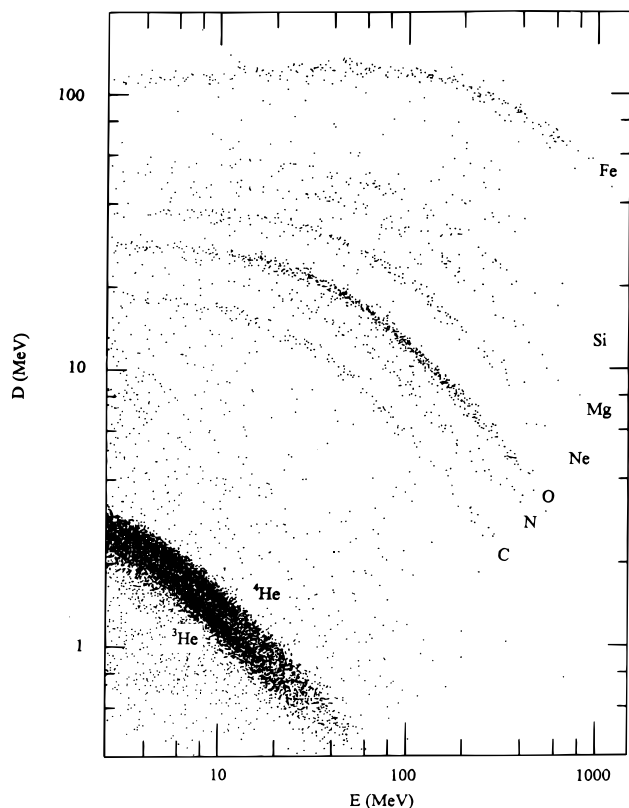


FIG. 1.—Pulse-height measurements in the *WIND/EPACT* LEMT telescope show energy deposit in the dome detector, “D,” vs. that in the “E” detector beneath it for individual particles during an impulsive-flare event. Tracks of representative element and isotope species of interest are identified in the figure.

troscopy cannot be used to determine spectra below  $\sim 1$  MeV, where we find a large fraction of the ion energy content to lie.

Higher quality direct measurements of ion spectra and abundances are essential, not only for understanding the physics of this dominant process of ion acceleration in flares, but also for understanding the production of nuclear-reaction secondaries such as  $\gamma$ -rays and neutrons that are strongly dependent on the nature of the ion beam as well as its energy spectrum.

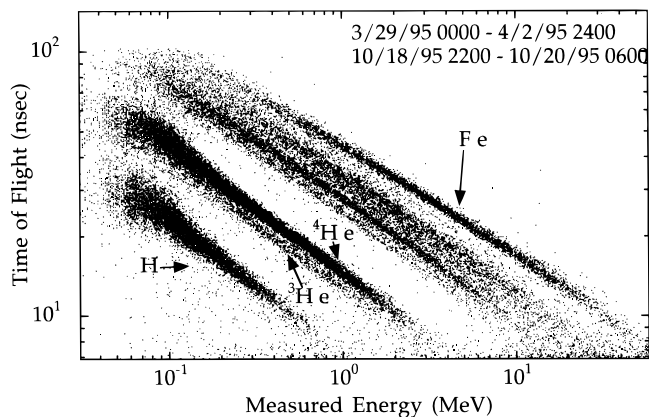


FIG. 2.—Pulse-height measurements in the *WIND/EPACT* STEP telescope show time-of-flight vs. energy for individual particles during a time period that includes impulsive-flare events. Tracks of representative element and isotope species of interest are identified in the figure.

Gradual events and their spatial and temporal relationship to the CME-driven shock wave have been studied most recently by Reames, Barbier, & Ng (1996) using multi-spacecraft measurements. Element abundances and spectra of H,  $^4\text{He}$ , C, O, and Fe above  $0.4 \text{ MeV amu}^{-1}$  were studied in gradual events by Mazur et al. (1992) and a review of abundances of 20 elements in  $\sim 50$  gradual events was presented by Reames (1995b).

## 2. INSTRUMENTATION

The Energetic Particles, Acceleration, Composition, and Transport (EPACT) experiment aboard the *WIND* spacecraft, launched 1994 November 1, has been described in some detail by von Rosenvinge et al. (1995). Within EPACT, the suprathermal energetic particle (STEP) system measures ion time-of-flight versus energy to resolve elements and isotopes of He in the  $\sim 20 \text{ keV amu}^{-1}$  to  $\sim 2 \text{ MeV amu}^{-1}$  region while the low-energy matrix telescope (LEMT) system uses  $dE/dx$  versus  $E$  techniques to resolve these same species from  $\sim 2$  to  $\sim 20 \text{ MeV amu}^{-1}$ . Geometry factors for the STEP and LEMT systems are  $0.8$  and  $51 \text{ cm}^2 \text{ sr}^{-1}$ , respectively. Figures 1 and 2 show the response of these two systems during representative periods studied in this paper.

The measurements from the *WIND/EPACT* Experiment are supplemented by high-energy measurements of H and He from the Goddard experiment aboard the *Interplanetary Monitory Platform 8 (IMP 8)* spacecraft (McGuire, von Rosenvinge, & McDonald 1986). This comparison is also important to provide a cross calibration between the recent measurements on *WIND* and the 23 yr history of measurements from the venerable *IMP 8* spacecraft.

## 3. TIME PROFILES AND VELOCITY DISPERSION

Impulsive-flare events often cluster together in time periods when the observer is magnetically connected to a flaring active region on the Sun. Several such periods have been identified during the *WIND* mission (Mazur, Mason, & von Rosenvinge 1996), even though solar events are usually quite small so near to solar minimum. For the present study we have selected events that occur in two time periods, in 1995 April and October. These are the only time periods during the first 1.5 yr of *WIND* data that contain individual impulsive events large enough to be seen by both the STEP and LEMT telescopes so that full spectra can be measured. In addition to the impulsive-flare events, the relatively large gradual event of 1995 October 20 is also studied.

Profiles of intensity versus time for  $^3\text{He}$  and Fe at two energies, separated by a factor of  $\sim 10$  in STEP and LEMT, are shown for the first study period in Figure 3. The events, indicated by numbers near their intensity maxima, show a rich variety of behavior. All four of the events are  $^3\text{He}$ -rich; however, event 1 is seen by LEMT but not by STEP, while event 4 is the largest event seen in  $^3\text{He}$  by STEP during this interval but is barely visible at the higher energies of LEMT. At LEMT energies, event 2 is seen as a sharp increase in  $^3\text{He}$  while event 3 is seen primarily by the sudden increase in Fe, 8 hr later. Event 3 would not have been recognized by  $^3\text{He}$  alone. As we move to the lower energies, event 2 fades rapidly into the background with only a small vestige surviving at the  $^3\text{He}$  energy shown, while event 3 is seen clearly in both  $^3\text{He}$  and Fe down to the lowest energies of STEP. A high Fe/O ratio during most of

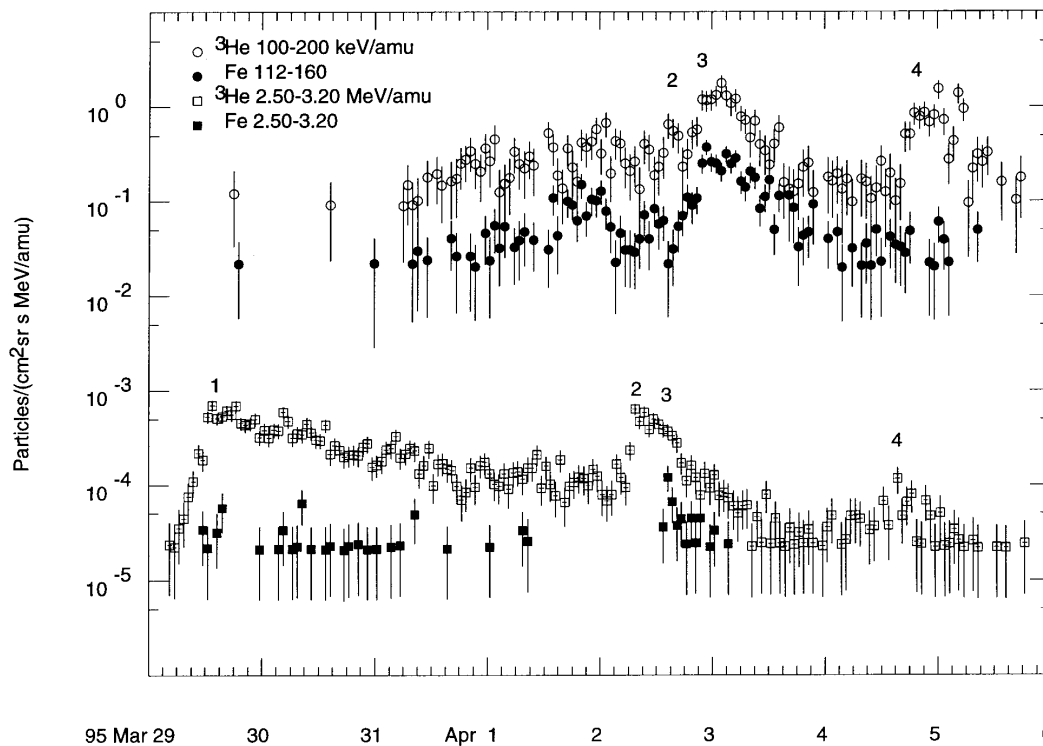


FIG. 3.—Profiles of intensity vs. time for  $^3\text{He}$  and Fe at two energies, separated by a factor of  $\sim 10$  and seen in *WIND/EPACT STEP* and *LEMT* telescopes during the first study period. The events discussed are indicated by numbers near their intensity maxima.

the event period (Mazur et al. 1996) suggests that “background” primarily consists of many smaller unresolved impulsive-flare events.

A delay of about 8 hr exists between the high- and low-energy ions shown in Figure 3 because of velocity dispersion. Velocity dispersion simply results because the time  $t$  required for particles of velocity  $v$  to propagate along a magnetic field line of length  $L$  is given by  $t = L/\mu v$ , where  $\mu$  is the cosine of the particle’s pitch angle with respect to the magnetic field. When  $L/\mu = 1$  AU, its minimum possible value, ions of 20 keV  $\text{amu}^{-1}$  still take 20 hr to begin to arrive from the Sun. Those of 1 MeV  $\text{amu}^{-1}$  take 2.9 hr, those of 100 MeV  $\text{amu}^{-1}$  take 18 minutes while photons or relativistic particles take only 8 minutes. If the particles suffer pitch-angle scattering and focusing during their transit, one can substitute  $\langle\mu\rangle$  for  $\mu$ , where the former is averaged over the trajectory. Studies of particle time profiles and angular distributions indicate that scattering mean free paths are  $\sim 1$  AU in these events (e.g., Mason et al. 1989).

The velocity dispersion of Fe ions in event 3 is shown in Figure 4; Fe ion energies range over 2 orders of magnitude in this figure. Large triangles in the figure mark the time of the flare and the expected onset time of each energy interval if  $L/\mu = 1.5$  AU. To determine energy spectra in an event such as this, we integrate over a time interval of fixed duration that begins at a time that depends upon the velocity dispersion for each velocity interval.

The interesting October time period is shown in Figure 5. Along with  $^3\text{He}$  and Fe, proton intensities from *LEMT* are shown to highlight particles accompanying the shock on October 18 and the onset of the large gradual event on October 20. The boundaries of a large flux-rope magnetic cloud (Burlaga et al. 1996) that represents a CME passing over the spacecraft are shown in the figure following the

primary shock and containing a small reverse shock. The  $^3\text{He}$  and Fe observations in and behind the cloud suggest the presence of several impulsive-flare events, but only one, indicated as event 5, is sufficiently large to permit spectral measurements. In the low-energy 56–80 keV  $\text{amu}^{-1}$  interval, Fe/O is  $\sim 1$  beginning early on October 19 and lasting until late on October 20. The event on October 20 begins at 0554 UT when a new, unrelated CME is launched at the Sun, as indicated by the type II and IV radio bursts of intensity 3. It is accompanied by an H $\alpha$  flare near W55°.

Particles from the large gradual event, event 6, suffer velocity dispersion just like those from impulsive events, except that  $L$  may decrease late in the event as the shock approaches Earth. However, since the intensities remain high at all energies because of the continuing acceleration by the shock, it is clearer to display this dispersion by normalizing intensities of all energies late in the event, as shown for  $^4\text{He}$  in Figure 6. Other ions behave in the same way as  $^4\text{He}$ . We are not aware of any previous report of such a universal decay curve lasting for several days, for all species, covering over 2 orders of magnitude in energy. This universality of the decay curve is a new feature of these observations. It may be related to the uniform spatial distributions seen at several energies behind the shock and CME as reported by Reames et al. (1996).

As seen in Figure 6,  $^4\text{He}$  ions in the lowest energy interval, 34–43 keV  $\text{amu}^{-1}$ , begin to arrive almost a day after the CME is launched at the Sun, and they reach an equilibrium intensity with the higher energy ions after another day has passed but still a day before the arrival of a weak shock at the spacecraft. However, one must remember that spatial, as well as temporal, variations are occurring. When the CME is launched at W55°, we are magnetically well connected to the nose of its shock, but when the shock arrives at 1 AU we are far around on its eastern flank, 55°

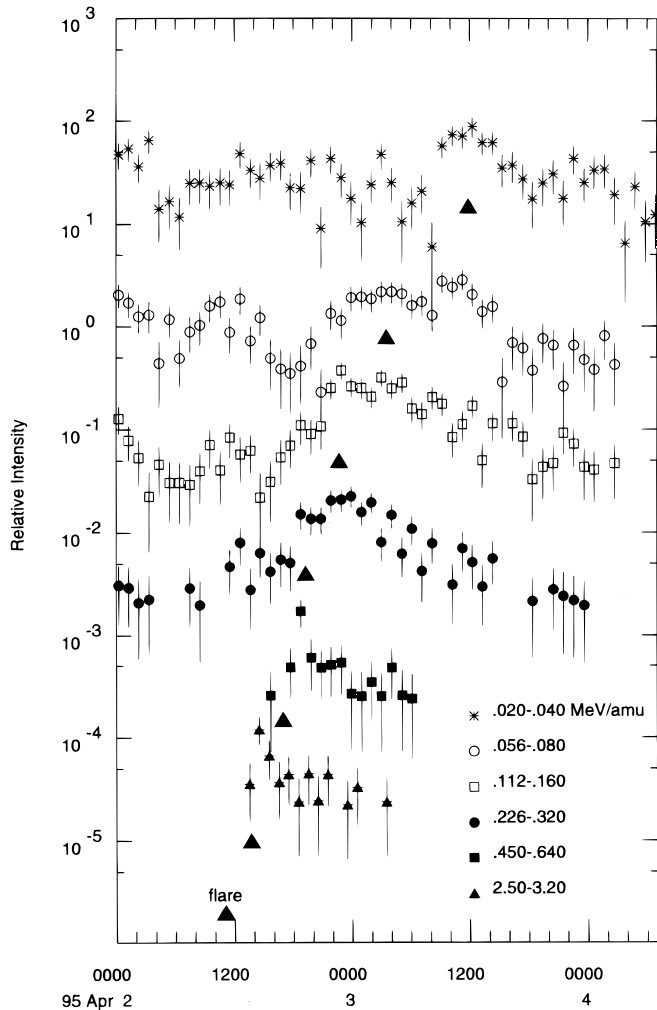


FIG. 4.—Velocity dispersion of Fe ions of different energy per nucleon (velocity) for event 3. The large triangles indicate the time of the flare and the expected delay at each energy (see text).

from the nose, where the shock is probably much weaker. Thus, when we see the  $34\text{--}43\text{ keV amu}^{-1}$  ions attain equilibrium with ions of higher energy, we have arrived on a field line  $\sim 40^\circ$  to the east of shock center on which all of the ions seen at that time were accelerated. However, there is abundant evidence from multispacecraft studies at widely separated longitudes that behind the shock the decrease in intensity is purely temporal (Reames et al. 1996). The time constant of that decay is 12.7 hr for the 1995 October 20 event (see Fig. 6).

#### 4. ENERGY SPECTRA

We begin by determining energy spectra for the large gradual event, where the most complete measurements are possible, and then turn to the impulsive events.

##### 4.1. Gradual Event Spectra

The energy-independent time profiles late in event 6, as seen in Figure 6, tell us that the energy spectral shape below  $\sim 10\text{ MeV amu}^{-1}$  at the shock does not vary in time (or shock longitude) during a 3 day period from the beginning of October 22 until October 25. Earlier in the event we cannot directly deduce the spectrum at the shock because some of the low-energy particles have not yet arrived from

it. However, it seems plausible to assume that the low-energy source spectrum is constant during early times as well. High-energy particles,  $> 10\text{ MeV amu}^{-1}$ , have returned to background intensities late in the event, but they are easily measured on October 21, for example. To obtain complete “source” spectra at the shock, we therefore combine high-energy spectra obtained on October 21 with the invariant low-energy spectra obtained after October 22, normalizing the two time intervals using the  $1\text{--}10\text{ MeV amu}^{-1}$   $^4\text{He}$  ions that are seen during the entire event period. The combined shock source spectra for H,  $^4\text{He}$ , C, O, and Fe are shown in Figure 7. These spectra depart little from a power-law shape over the entire  $\sim 20\text{ keV amu}^{-1}$  to  $\sim 100\text{ MeV amu}^{-1}$  region. Power-law spectra are expected theoretically for shock acceleration below  $\sim 30\text{ MeV amu}^{-1}$  (Ellison & Ramaty 1985). We should note that other observations (e.g., Reames et al. 1996) in larger events suggest that efficiency for acceleration of high-energy ions ( $> 30\text{ MeV amu}^{-1}$ ) may decrease more rapidly than those at low energies as the shock expands outward from the Sun; we are unable to observe that effect in this event, perhaps because of the relatively steep spectra.

It is important to realize that alternative techniques for deducing spectra in gradual events artificially produce spectra that are rounded at low energies because they bias against low-energy particles. Integrating throughout the entire event biases against low-energy particles since it includes time periods before they have arrived. Time-of-maximum spectra for well-connected events, prescribed by the old diffusion models, bias against low-energy particles since low-energy particles arrive later when intensities of all species may be reduced at the shock, partly because the observer is now magnetically connected far around on its eastern flank. It is the existence of invariant spectra at low energies that allows us to develop a technique that can circumvent this bias against low-energy ions.

##### 4.2. Impulsive-Flare Spectra

Ion spectra for events 3 and 5 are shown in Figure 8. In each case, ions from the event can be distinguished from the background down to the lowest energies, as was shown in Figure 4. Note, however, that C and O are poorly resolved by STEP at its lowest and highest observable energy. Also, above  $\sim 5\text{ MeV amu}^{-1}$  the spectra of  $^4\text{He}$  and O are dominated by the anomalous cosmic rays (ACRs). The spectra of most of the ions tend to be much more rounded than those in the gradual event, their slope steepening with increasing energy. The spectra of  $^3\text{He}$  and  $^4\text{He}$  have different slopes at lower energies so that  $^3\text{He}/^4\text{He}$  decreases toward lower energies; however, we should note that low-energy background from corotating interaction regions (CIRs) might be more important for H and  $^4\text{He}$  than for the other ions. Rounded, Bessel-function spectra are a property of stochastic acceleration (Forman, Ramaty, & Zwebel 1986) and were previously observed down to  $0.4\text{ MeV amu}^{-1}$  by Möbius et al. (1982), to  $0.1\text{ MeV amu}^{-1}$  by Reames et al. (1992), and to  $0.3\text{ MeV amu}^{-1}$  by Mazur et al. (1995). However, the theoretical spectral shapes of Möbius et al. (1982) do not fit our observations over the full range of energies for any species except possibly H. The observed spectra are harder at high energies than the Bessel-function forms.

Event-to-event spectral variations are shown in Figure 9 where the impulsive-flare spectra in the five events are com-

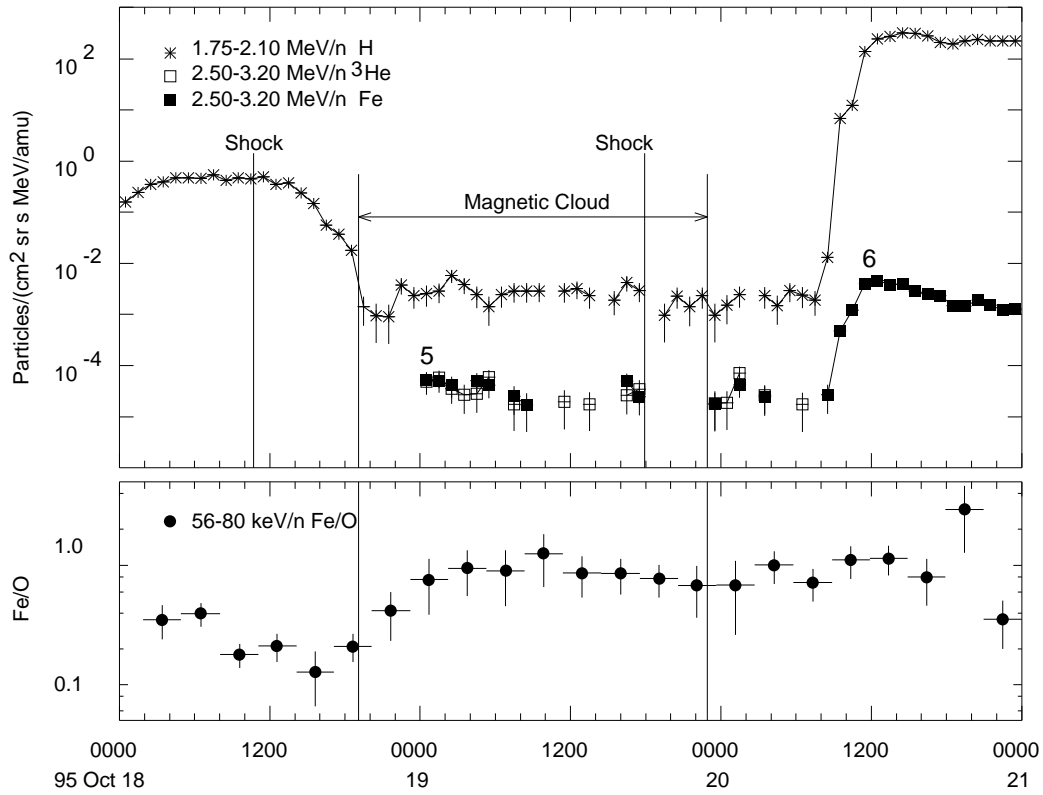


FIG. 5.—Intensities of H,  $^3\text{He}$ , and Fe during the second study period are shown in the upper panel for the 1995 October period. Note the presence of  $^3\text{He}$  and Fe inside the magnetic cloud. The lower panel shows  $\text{Fe}/\text{O} \sim 1$  in and behind the cloud at  $56\text{--}80 \text{ keV amu}^{-1}$ . The high value of  $\text{Fe}/\text{O}$  probably results from many unresolved impulsive-flare events.

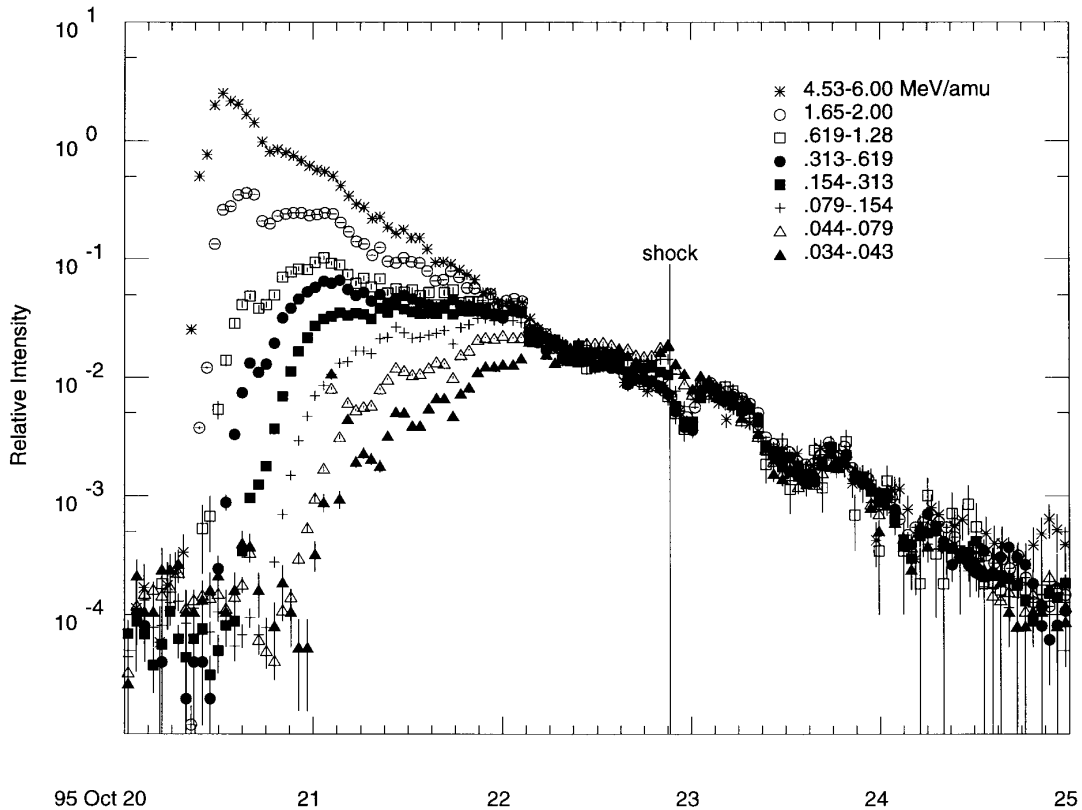


FIG. 6.—Profiles of intensity vs. time for hourly averaged  $^4\text{He}$  from  $34 \text{ keV amu}^{-1}$  to  $4 \text{ MeV amu}^{-1}$  normalized during the energy-invariant period late in gradual event 6 of 1995 October 20. Characteristic velocity dispersion is seen during the rise phase of successively lower energy particles. The time of passage of a weak shock is shown. Time profiles of other species (not shown) have a similar behavior.

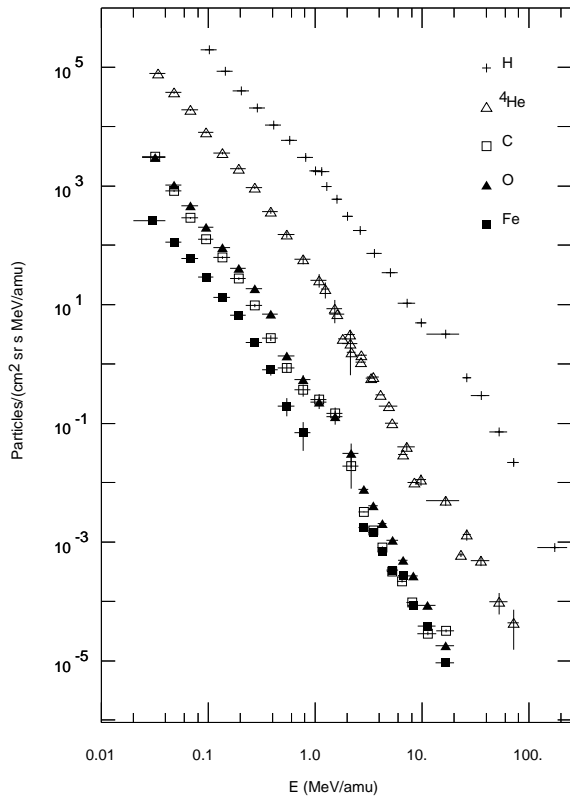


FIG. 7.—Invariant shock “source” spectra for H,  $^4\text{He}$ , C, O, and Fe during gradual event 6 of 1995 October 20 (see text). H and He observations from *IMP 8* are included with those from STEP and LEMT to produce these spectra. Note the C and O are not resolved by STEP near its highest ( $>1 \text{ MeV amu}^{-1}$ ) and lowest ( $<50 \text{ keV amu}^{-1}$ ) energies.

pared for  $^3\text{He}$  and for Fe. The lower energy Fe points should be treated as upper limits in events 1, 2, and 4, since Fe from the flares cannot be distinguished unambiguously from the background Fe-rich material in these cases. Power-law spectral indices show a wide range from  $-1.8$  to  $-3.4$  in these events, although the spectra are not well represented as either power laws or Bessel functions.

5. CONCLUSIONS

We have shown that energy spectra from  $\sim 0.02$  to  $\sim 5 \text{ MeV amu}^{-1}$  in the gradual event of 1995 October 20 have time-invariant power-law form for a  $\sim 3$  day period if we wait sufficiently late in the event for the low-energy particles to have time to propagate to 1 AU. This invariance allows us to determine the spectra (without the bias against low-energy particles that is present in event-averaged spectra or in time-of-maximum spectra) for a particle population that is decreasing with time (see Reames et al. 1996).

It has been known for some time that impulsive-flare particles are seen during clusters of events that occur when the observer is magnetically connected to an active region (Reames et al. 1985, 1988). Often these events are seen in the region behind a CME (Kahler & Reames 1991). In this paper we have reported events that occur inside a magnetic flux rope that represents magnetic field ejected with the CME. It is only because of the high sensitivity of EPACT that these events are seen, since they are much too small to have been detected by instruments flown during previous decades.

Cliver (1996) has suggested that the magnetic reconnection at the Sun behind a CME can lead to flaring and particle acceleration under conditions similar to those in

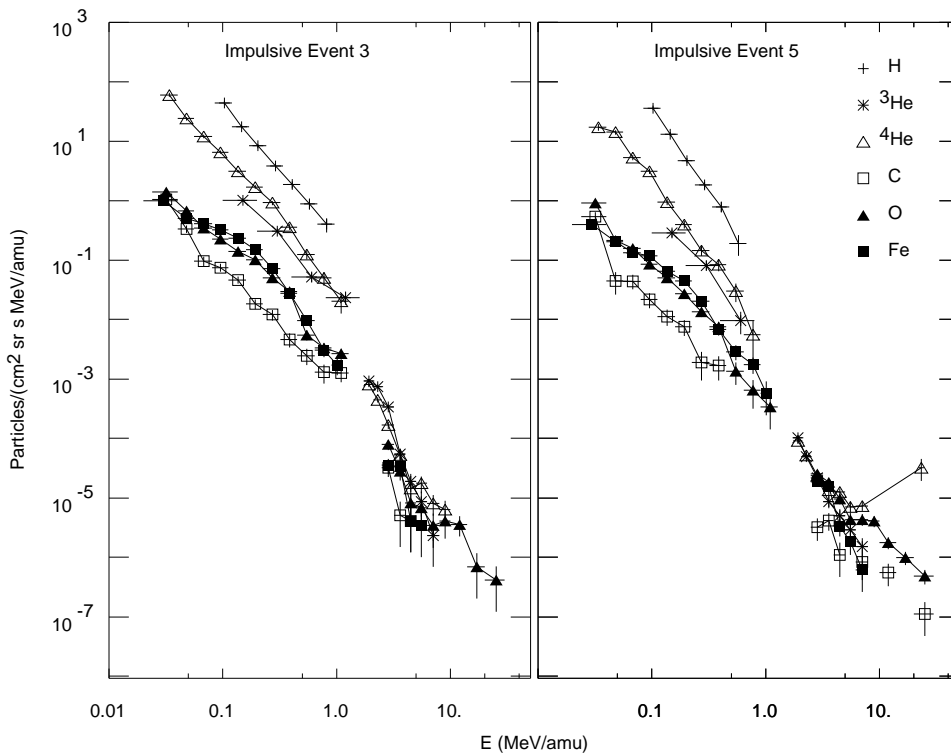


FIG. 8.—Energy spectra of H,  $^3\text{He}$ ,  $^4\text{He}$ , C, O, and Fe in impulsive-flare events 3 and 5. Note that C and O are not well resolved at the lowest and highest energies observed by STEP.

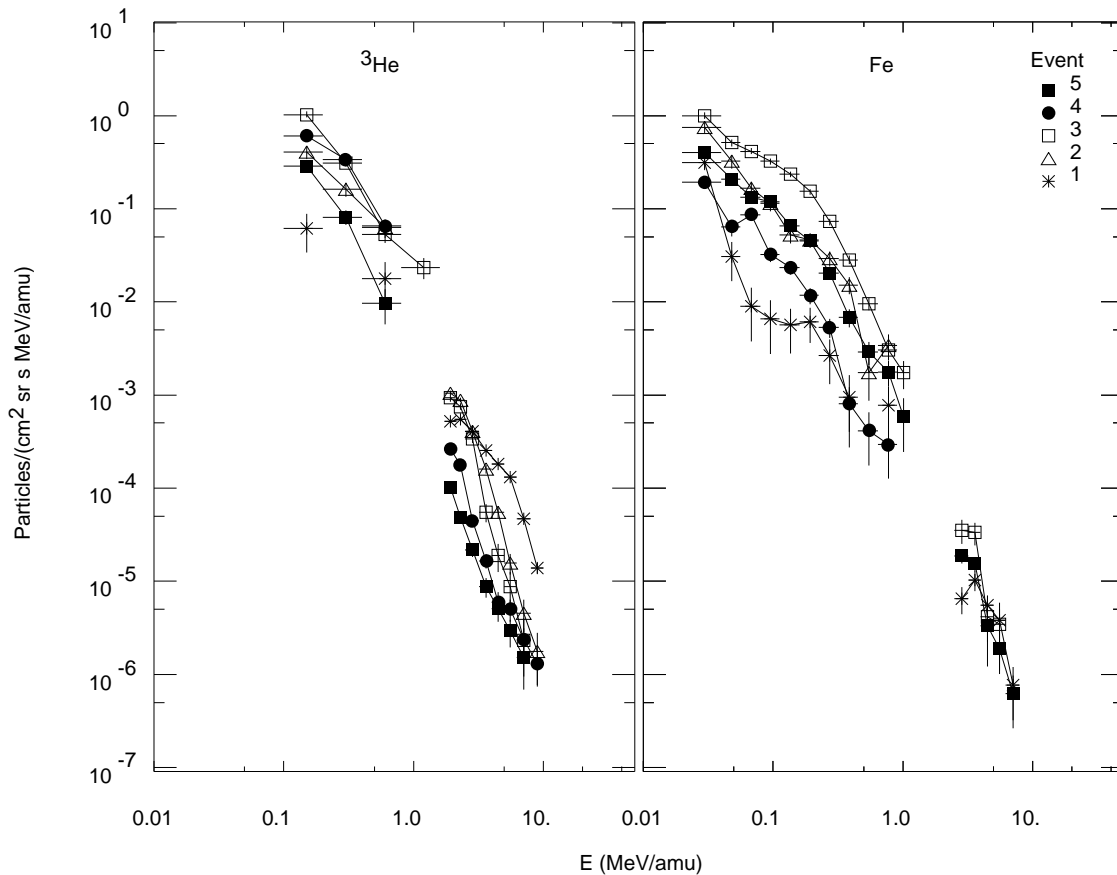


FIG. 9.—Comparative energy spectra for  ${}^3\text{He}$  (left panel) and for Fe (right panel) for all five impulsive-flare events (see text). The spectra are not well represented by either power laws or Bessel functions.

discrete impulsive flares. In any case it is true that, in the region behind a CME, one can find field lines that connect to an active region where impulsive flares occur (independently of what caused them to occur). Especially near solar minimum, most of interplanetary space is filled with field lines that have diverged out of coronal holes where impulsive flares do not occur. Hence, the clustering of impulsive-flare particle events behind CMEs may be only a consequence of a favorable magnetic topology in that region.

The energy spectra in impulsive-flare events, especially those of  ${}^3\text{He}$  and the heavy elements, are much more rounded than those we obtained for the gradual event, the spectra steepening with increasing energy. Rounded spectra have been noted previously in impulsive events (Möbius et al. 1982) over a more limited energy range and are attributed to stochastic acceleration by wave-particle interactions in Alfvén turbulence. However, the specific model of Möbius et al. (1982) does not fit our observations over the full energy range, and, of course, we now understand that wave modes other than Alfvén waves are required to produce the enhancement of  ${}^3\text{He}$  (e.g., Temerin & Roth

1992). Complete spectral calculations are not yet available from more recent theories such as the theory of cascading waves (Miller & Reames 1996). The steeper spectra for H and  ${}^4\text{He}$ , also noted by Möbius et al. (1982), may also be a property of the events, but these two species may be affected by a larger contribution of CIR background at lowest energies. We are unlikely to resolve this situation until we are able to see larger, clearer impulsive events that will become more common as we approach solar maximum.

While the impulsive-flare spectra do flatten at low energies, it is important to stress that they do continue to rise down to energies of  $20 \text{ keV amu}^{-1}$ , far below the energy of the  $1.63 \text{ MeV } \gamma\text{-ray}$  line of Ne. This low-energy portion of the spectrum should be considered as a significant contribution to the total energy content of ions in flares (Ramaty et al. 1996). Particle intensities at  $20 \text{ keV amu}^{-1}$  can be a factor of  $10^5$  higher than those at  $1 \text{ MeV amu}^{-1}$ .

We thank James A. Miller for his comments on this manuscript. This work was supported in part by NASA contract NAS 5-30927, and grant NAG 5-2865.

#### REFERENCES

- Burlaga, L., Lepping, R. P., Mish, W., Ogilvie, K. W., Szabo, A., Lazarus, A. J., & Steinberg, J. T. 1996, *ApJ*, submitted  
 Cliver, E. W. 1996, in *AIP Conf. Proc. 374, High Energy Solar Physics*, ed. R. Ramaty, N. Mandzhavidze, & X.-M. Hua (New York: AIP), 45  
 Ellison, D. C., & Ramaty, R. 1985, *ApJ*, 298, 400  
 Forman, M. A., Ramaty, R., & Zweibel, E. G. 1986, in *Physics of the Sun*, ed. P. A. Sturrock, vol. 2 (Dordrecht: Reidel), 249  
 Gosling, J. T. 1993, *J. Geophys. Res.*, 98, 18949  
 Kahler, S. W., & Reames, D. V. 1991, *J. Geophys. Res.*, 96, 9419  
 Mason, G. M., Ng, C. K., Klecker, B., & Green, G. 1989, *ApJ*, 339, 529

- Mason, G. M., Reames, D. V., Klecker, B., Hovestadt, D., & von Rosenvinge, T. T. 1986, *ApJ*, 303, 849
- Mazur, J. E., Mason, G. M., & Klecker, B. 1995, *ApJ*, 448, L53
- Mazur, J. E., Mason, G. M., Klecker, B., & McGuire, R. E. 1992, *ApJ*, 401, 398
- Mazur, J. E., Mason, G. M., & von Rosenvinge, T. T. 1996, *Geophys. Res. Lett.*, 23, 1219
- McGuire, R. E., von Rosenvinge, T. T., & McDonald, F. B. 1986, *ApJ*, 301, 938
- Miller, J. A., & Reames, D. V. 1996, in *AIP Conf. Proc. 374, High Energy Solar Physics*, ed. R. Ramaty, N. Mandzhavidze, & X.-M. Hua (New York: AIP), 450
- Miller, J. A., & Viñas, A. F. 1993, *ApJ*, 412, 386
- Möbius, E., Scholer, M., Hovestadt, D., Klecker, B., & Gloeckler, G. 1982, *ApJ*, 259, 397
- Murphy, R. J., Ramaty, R., Kozlovsky, B., & Reames, D. V. 1991, *ApJ*, 371, 793
- Ramaty, R., Mandzhavidze, N., Kozlovsky, B., & Murphy, R. J. 1995, *ApJ*, 455, L193
- Reames, D. V. 1990, *ApJS*, 73, 235
- . 1993, *Adv. Space Res.*, 13(9), 331
- . 1995a, *Revs. Geophys. Suppl.*, 33, 585
- . 1995b, *Adv. Space Res.*, 15(7), 41
- Reames, D. V., Barbier, L. M., & Ng, C. K. 1996, *ApJ*, 466, 473
- Reames, D. V., Cane, H. V., & von Rosenvinge, T. T. 1990, *ApJ*, 357, 259
- Reames, D. V., Dennis, B. R., Stone, R. G., & Lin, R. P. 1988, *ApJ*, 327, 998
- Reames, D. V., Meyer, J. P., & von Rosenvinge, T. T. 1994, *ApJS*, 90, 649
- Reames, D. V., Richardson, I. G., & Wenzel, K.-P. 1992, *ApJ*, 387, 715
- Reames, D. V., & Stone, R. G. 1986, *ApJ*, 308, 902
- Reames, D. V., von Rosenvinge, T. T., & Lin, R. P. 1985, *ApJ*, 292, 716
- Share, G. H., & Murphy, R. J. 1995, *ApJ*, 452, 933
- Temerin, M., & Roth, I. 1992, *ApJ*, 391, L105
- Van Hollebeke, M. A. I., McDonald, F. B., & Meyer, J. P. 1990, *ApJS*, 73, 285
- von Rosenvinge, T. T., et al. 1995, *Space Sci. Rev.*, 71, 155
- Zhang, T. X. 1995, *ApJ*, 449, 916
- Zhang, T. X., & Ohsawa, Y. 1995, *Sol. Phys.*, 158, 115